

Numerical Simulation of Liquid Jets Impinging on an Isothermal Stationary Substrate and Hydraulic Jump

Md. Masbah-Ul-Hakim¹, Zahir U. Ahmed¹

¹Department of Mechanical Engineering, Khulna University of Engineering & Technology, Khulna-9203, Bangladesh

E-mail: zuahmed@me.kuet.ac.bd, masbah.067@gmail.com

Abstract

The main objective of this paper is to investigate the fluid flow behavior of liquid jets impinging on an isothermal flat surface and characterization the hydraulic jump. In this regard, numerical simulations were performed on 2D axisymmetric jets using ANSYS Fluent v18.0 for a specific flow velocity equal to 2 m/s. Level set volume of fluid (VOF) method with compressive scheme was implemented to track the free surface of the jet. The location and height of the hydraulic jump have been determined and compared with the experimental data in order to validate the model. The results show a maximum deviation of 4% for hydraulic jump location with the existing results in literature. Velocity vector at the stagnation zone, pressure coefficient, axial and radial velocity of the jet and turbulent kinetic energy of the fluid flow domain were then presented. Maximum static pressure was found to be 2108.28 Pa at the stagnation point which decreases radially from that point. Both the radial and axial velocity were found zero at the stagnation point.

Keywords: impinging jet, stationary surface, hydraulic Jump.

1. Introduction

Impingement of liquid jets is one of the most effective mechanism through which high rates of convective heat and mass transfer can be achieved when a fluid jet strikes a solid surface. As the boundary layer is very thin and flow velocity is high around the impingement region, heat can be dissipated very efficiently [1]. In different industrial processes, impingement of liquid jets phenomenon is used such as cooling of electronic devices, piston and turbine blades, sheet metal processing in manufacturing, generator coils, laser mirrors, glass tempering, drying and freezing [2]. There are three configurations of impinging jets available such as free jet, submerged jet and confined submerged jet. Free-surface jets use dense fluid in a lighter fluid (e.g. liquid in air), submerged jets offer impingement of fluid in the same fluid medium (e.g. air in air) and confined submerged jets are similar to submerged jet but allow confining the wall. In this regard, shape of the free surface jet is affected by the gravitational force, surface tension and pressure forces. On the other hand, the forces are affected by the size, shape and speed of the jet. In this paper, free surface liquid jets in stationary air will be considered.

Previous experimental and analytical treatises on this topic had collected a volume of information to understand fundamental physics. Early efforts were primarily focused on the formation of hydraulic jump due to impingement of a single jet onto a flat rigid surface. The flow pattern, formed due to impingement of liquid stream vertically over the flat surface was outlined by Arakeri and Rao [3]. Avedisian and Zhao [2] carried out the effect of gravity on the radius of the jump using drop tower. Bush and Aristoff [4] provided a shift in the radial location of the jump over a surface when the surfactant is mixed with impinging water. Prince et al. [5] developed an analytical model for the jump with consideration of slip over the surface and identified a rise in the jump radius for a moving impingement surface. On a similar note, researchers showed that impingement of oblique jet onto the solid flat surface, in comparison to normal impact, exhibits an azimuthally asymmetric profile of hydraulic jump. Kibar et al. [6] carried out an experiment to investigate the formation of the jump due to oblique impact on hydrophobic and super-hydrophobic surfaces. Kate et al. [7] analyzed that the circular hydraulic jump changes its shape if the jet inclination is changed through 90 degrees. Elliptical jumps would form if the jets inclination angle varied between 0 to 90 degrees. Kasimov [8] considered the flow over a flat plate of finite radius and investigated the fluid flow structure upstream and downstream of the jump. He used far-field boundary conditions involving the effect of surface tension to determine the hydraulic jump location. Computational simulation of radially asymmetric hydraulic jumps and jump-jump interactions was observed by Singh and Das [9]. Cho et al. [10] also

carried out a three-dimensional numerical study of impinging water jets in runout table to observe the flow phenomena and cooling rate.

In recent days, Duchesne et al. [11] found that the Froud number is constant after the jump which is independent of flow rate, viscosity and surface tension. Mohajer et al [12] found that the Froud number after the impingement is constant and independent of flow rate though the inner Froud number changes due to surface tension of the flowing fluid. They also investigated the maximum and minimum outer and inner Froud number theoretically and found that the outer Froud number could be more than unity depending on surface tension. Choo and Kim [13] experimentally observed that the dimensionless hydraulic jump radius does not depend on jet diameter when there are constant impingement power phenomena. They also developed a relation for the hydraulic jump radius which was a function of the impingement power only. Using water and ethylene glycol as the working fluid, Todkari and Kate [14] investigated the circular hydraulic jump due to normal impingement both numerically and experimentally. They forged a small hole in the impingement region to observed the flow phenomena of this modified flow region.

The study of impinging jet and hydraulic jump has been a great concern among researchers over the years. In comparison with the previous approach, numerical observation received a little concern. Previous numerical works [10, 15-16] were solved by trial and error methods by assuming the location of free surface only. Present study is carried out by using the volume of fluid method to capture the interface. This method is more robust than previously used methods to track the free surface. As a result, highly accurate computation can be achieved. On the other hand, surface tension phenomena are also included in this study which has not considered properly in previous models.

2. Numerical Methodology

The equations govern the flow are steady incompressible conservations of mass and momentum. Analysis of turbulent flow is usually performed by using Reynolds Averaged Navier-Stokes equation (RANS) model in commercially available software package ANSYS Fluent v18. The main advantage of RANS model is that it takes less computational time than the time accurate equations as well as large scale eddy simulation. The resulting RANS equations for the problem are [17]:

$$\frac{\partial \rho}{\partial t} + \frac{\partial(\rho \bar{u}_i)}{\partial x_i} = 0 \quad (1)$$

$$\frac{\partial(\rho \bar{u}_i)}{\partial t} + \frac{\partial(\rho \bar{u}_i \bar{u}_j)}{\partial x_j} = -\frac{\partial \bar{p}}{\partial x_i} + \frac{\partial}{\partial x_j} \left[\mu \left(\frac{\partial \bar{u}_i}{\partial x_j} + \frac{\partial \bar{u}_j}{\partial x_i} - \frac{2}{3} \delta_{ij} \frac{\partial \bar{u}_k}{\partial x_k} \right) \right] + \frac{\partial(-\rho \bar{u}_i \bar{u}_j)}{\partial x_j} \quad (2)$$

The Boussinesq hypothesis can be used to make a relationship between Reynolds stress term ($\rho \bar{u}_i \bar{u}_j$) and the mean velocity gradients which is as follows:

$$-\rho \bar{u}_i \bar{u}_j = [\mu_t \left(\frac{\partial \bar{u}_i}{\partial x_j} + \frac{\partial \bar{u}_j}{\partial x_i} \right) - \frac{2}{3} (\rho k + \mu_t \frac{\partial \bar{u}_k}{\partial x_k}) \delta_{ij}] \quad (3)$$

Here μ_t is the viscosity for turbulence and k is turbulent kinetic energy. For all our simulations, k- ω based Shear-Stress-Transport (SST) model [18] is used to solve turbulence as it provides good predictions boundary layer simulation and of the onset and the amount of flow separation by the inclusion of transport effects into the formulation of eddy viscosity. The k- ω models assume that the turbulence viscosity is related to the turbulence kinetic energy by:

$$\mu_t = \rho \frac{k}{\omega} \quad (4)$$

The k- ω models solve two equations as follows [19].

$$\frac{\partial \rho k}{\partial t} + \frac{\partial(\rho u_j k)}{\partial x_j} = \frac{\partial}{\partial x_j} \left[\left(\mu + \frac{\mu_t}{\sigma_k} \right) \frac{\partial k}{\partial x_j} \right] + p_k - \beta' \rho k \omega + p_{kb} \quad (5)$$

$$\frac{\partial(\rho \omega)}{\partial t} + \frac{\partial(\rho u_j \omega)}{\partial x_j} = \frac{\partial}{\partial x_j} \left[\left(\mu + \frac{\mu_t}{\sigma_\omega} \right) \frac{\partial \omega}{\partial x_j} \right] + \alpha \frac{\omega}{k} p_k - \beta \rho \omega^2 + p_{wb} \quad (6)$$

Here p_k is the production rate of turbulence.

The free surface flow in water jet impingement is captured by volume of fluid (VOF) method. It mainly finds the control volumes that contain the interface depending on the value of volume fraction of liquid. If the value of volume fraction is 0 then the cell contains no liquid, if the value is 1 then the cell is full of liquid and if the value is between 0 to 1 then the interface is in that cell. For our simulations, implicit volume fraction parameters formulation with Level-Set method is used to solve VOF equation [20]:

$$\frac{1}{\rho_q} \left[\frac{\partial(\alpha_q \rho_q)}{\partial t} + \nabla \cdot (\alpha_q \rho_q \vec{v}_q) \right] = S_{\alpha_q} + \sum_{p=1}^n (\dot{m}_{pq} - \dot{m}_{qp}) \quad (7)$$

\dot{m}_{pq} is the transfer of mass from phase p to q, \dot{m}_{qp} is the transfer of mass from phase q to p and S_{α_q} is the source term and ρ_q is density for q phase. Along with the VOF method, the surface tension model is also used which results in a source term in the conservation of momentum equation.

Figure 1 presents the 2-D axisymmetric geometry, where the axis of symmetry is taken as x axis and the flat stationary plate is considered in y axis. A steady incompressible liquid jet with radius 1 mm impinging on a stationary smooth surface at a volume flow rate Q is considered. The plate has a radius of 50 mm and is centered on the impact point of the jet. The distance between the nozzle and the plate is 10 mm.

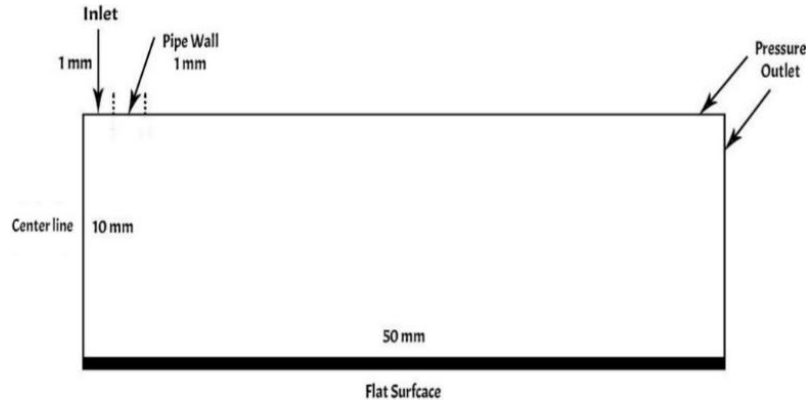


Fig. 1. Geometry of the 2-D axisymmetric case.

Quadrilateral cell type was used for meshing and very fine uniform mesh was developed near the boundary to obtain better accuracy. The number of meshed elements was 86400 and number of nodes was 87001 with minimum orthogonal quality very close to 1, indicating a good mesh quality for the simulation. The liquid entering into the computational domain through the inlet having uniform velocity 2 m/s. Pressure outlet is considered for the outlet and no slip condition is applied for the solid surface or wall. For this case, taking $\mu=8.90 \times 10^{-4}$ Pa.s, $g = 10$ m/s, $\gamma = 0.07$ N/m, $P = 101325$ Pa and $\rho = 1.225$ kg/m³. For the simplification of the calculation, the flow is assumed to be symmetric in the midplane.

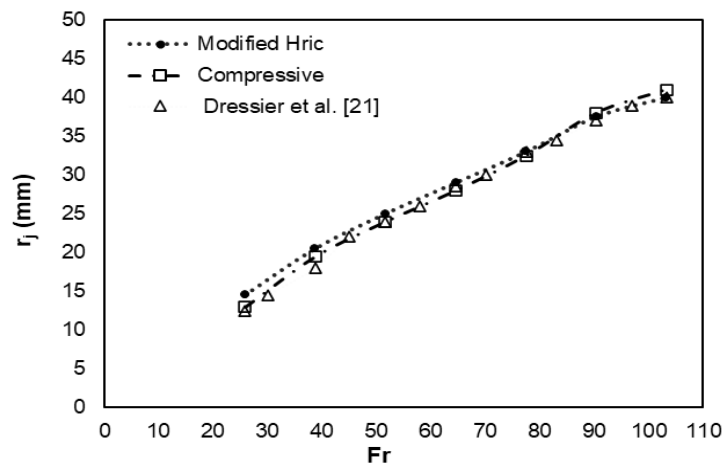


Fig. 2. Dependence of hydraulic jump location on flow rate (Froud Number).

In order to validate our present work, the results of numerical simulations for two different volume fraction schemes, namely, ‘Compressive scheme’ and ‘Modified HRIC scheme’ are tested first in order to identify the best performing scheme. In this regard, the location of the hydraulic jump for different flow rates (expressed in terms of Froud number) obtained from the simulations is compared with the measurements of Dressaire et al. [21], as shown in figure 2. According to the measurement, for Froud number 25.82, the hydraulic jump on the plate occurred at 12.5 mm away from the stagnation point. Results found from the simulation show that, for Compressive scheme, jump occurs at 13 mm and for Modified HRIC, jump occurs at 14.5 mm. The difference between the experimental value and Compressive value is 3.84% and the value is 13.79% for Modified HRIC. As such, compressive scheme is found to be better agreement with the experimental data. Thus, later investigations were conducted using compressive scheme.

3. Results and discussion

The free surface flow was simulated by using the VOF method and the interfaces between air and water for jet velocity 2 m/s are shown in figure 3. It is clear from Figure 3 that the radius of hydraulic jump is 19.5 mm from

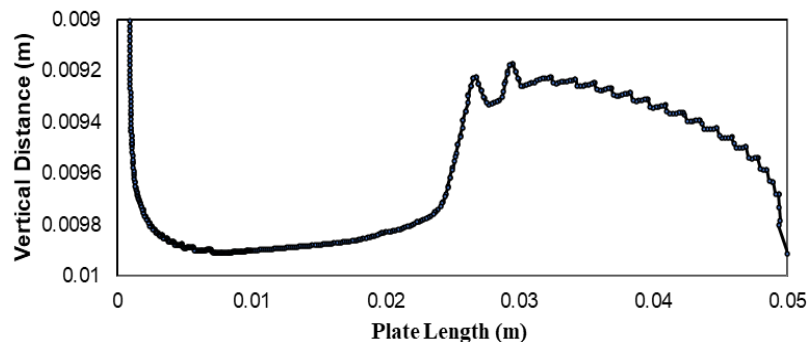


Fig. 3. Shape of the interface for 2 m/s water jet velocity.

the impinging point. The liquid film thickness for jet velocity 2 m/s is 0.001 mm which is very thin. The highest pressure occurs at the stagnation point which is just below the jet nozzle where the velocity also diminishes. Due to this high pressure, the liquid spreads parallel to the flat surface.

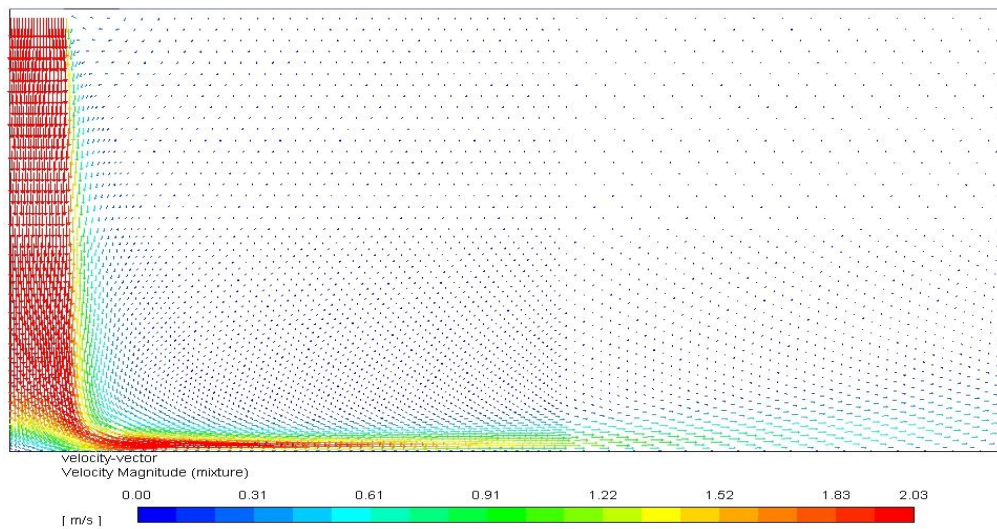


Fig. 4. Velocity vector plot at 2 m/s.

At the stagnation zone, most of the changes occur such as shear stress is created by the velocity gradient which results in high heat and mass transfer according to Reynolds analogy. There is very thin boundary layer at the stagnation zone which grows as the liquid moves parallel to the surface from the impinging point. The flow characteristics due to jet impingement can be understood from figure 4 which shows the velocity vector plot at 2 m/s.

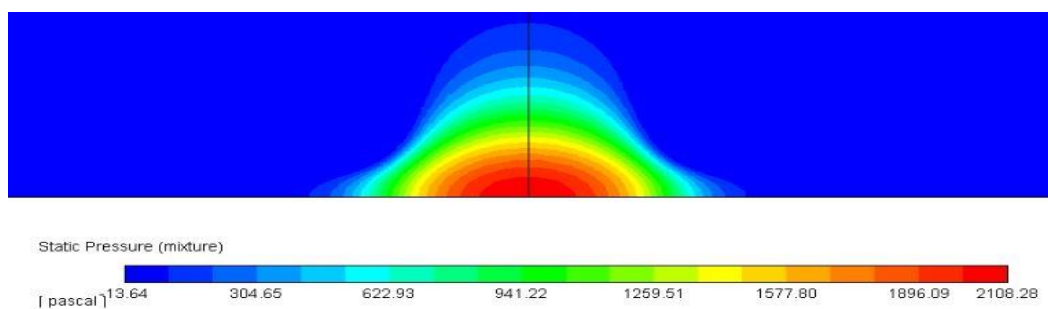


Fig. 5. Contour of static pressure for nozzle velocity 2 m/s.

Figure 5 to figure 8 show different flow characteristics of impinging jet on a stationary surface. Figure 5 illustrates the static pressure which reaches to a maximum value of 2108.28 Pa at the stagnation point and decreases close to zero radially from the impinging point. Generally, the nonzero pressure region is known as stagnation region. The change of pressure at stagnation zone is faster with larger variation of the jet inlet velocity which also narrow the stagnation zone.

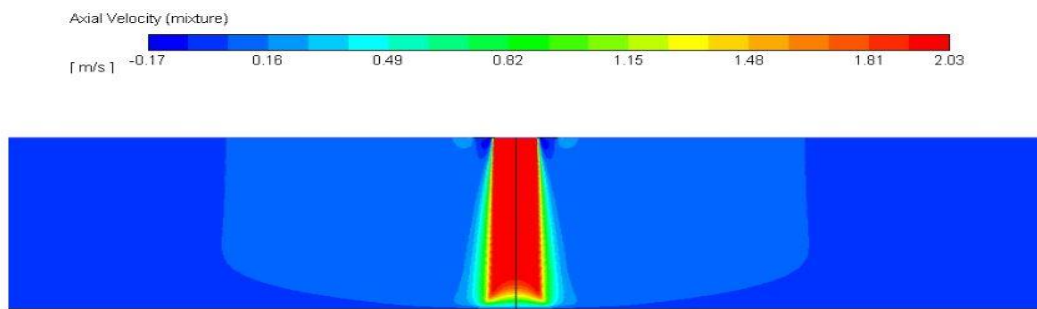


Fig. 7. Contour of axial velocity for nozzle velocity 2 m/s

The axial and radial velocity profile for nozzle exit velocity 2 m/s are shown in figure 7 and figure 8 respectively. Both the axial and radial velocity are zero at the stagnation point which is an important characteristic of jet impingement phenomenon. The radial velocity is equal to the nozzle exit velocity just beside the stagnation point which decreases in radial direction.

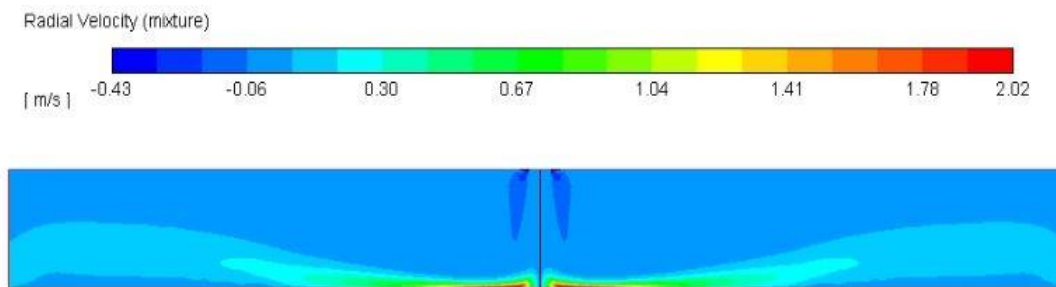


Fig. 8. Contour of radial velocity for nozzle velocity 2 m/s.

Turbulent kinetic energy predicted by the turbulence models is graphically represented in figure 9 at various locations of the fluid flow domain for the nozzle to plate spacing $H/D=5$. At the stagnation point where $r/D=0$, the $k-\omega$ models predicted the turbulent kinetic energy as $106 \text{ mm}^2/\text{s}^2$. This value increases sharply to $182 \text{ mm}^2/\text{s}^2$ at a small distance from the stagnation point. Then the turbulent kinetic energy decreases gradually and reaches approximately to 0 at a distance 0.015 m from the impingement point. It remains zero for the rest of the fluid flow domain.

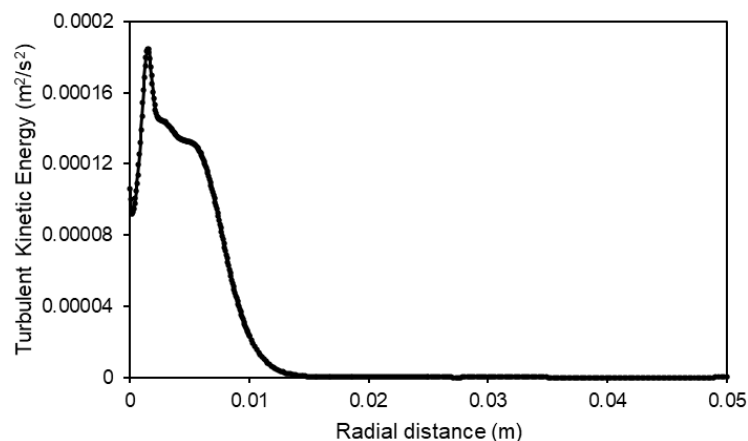


Fig. 9. Turbulent kinetic energy predicted by $k-\omega$ models at the various locations at 2 m/s jet velocity.

4. Conclusion

In this study, numerical investigations were done on impinging jet on a stationary surface for 2 m/s jet velocity and various jet characteristics were investigated by solving continuity and momentum equation using VOF method. The effects of flow rate on hydraulic jump location are observed in order to validate the simulation and found a close agreement with the experimental results. It has been observed that the liquid film thickness after the impingement is very thin and increases markedly, attaining a maximum thickness representing the hydraulic jump formation. Then the film thickness falls gradually at the downstream region of the hydraulic jump. The location and height of hydraulic jump have been obtained and different characteristics of impinging jet such as pressure, axial and radial velocity have analyzed. Turbulence modeling based on SST $k-\omega$ model has shown that the results are quite good in comparison. In real practice, the plate is not stationary but a continuously moving object. Hence, a study of two phase flow heat transfer with moving surface phenomenon can be introduced in future.

5. References

- [1] J. H. Lienhard V, "Heat transfer by impingement of circular free-surface liquid jets" (18th National and 17th ISHMT-ASME Conference IIT Guwahati, India, 2006) pp. k206–k221.
- [2] C. T. Avedisian, Z. Zhao, "The circular hydraulic jump in low gravity" (In Proceedings of the Royal Society of London A: Mathematical, Physical and Engineering Sciences, 2000) pp. 2127-2151.
- [3] J. H. Arakeri, K. A. Rao, "On radial film flow on a horizontal surface and the circular hydraulic jump," (Journal of Indian Institute of Science, 1996) pp.73-91.
- [4] J. W. M. Bush, J. M. Aristoff, "The influence of surface tension on the circular hydraulic jump" (Journal of Fluid Mechanics) pp. 33-52.
- [5] J. F. Prince, D. Maynes, J. Crockett J "Analysis of laminar jet impingement and hydraulic jump on a horizontal surface with slip" (Physics of Fluids 24, 2012)
- [6] A. Kibar, H. Karabay, K. S. Yiğit, I. O. Ucar, H. Y. Erbil, "Experimental investigation of inclined liquid water jet flow onto vertically located superhydrophobic surfaces" (Experiments in Fluids, 2010) pp. 1135-1145.
- [7] R. P. Kate, P. K. Das, S. Chakraborty, "An investigation on non-circular hydraulic jumps formed due to obliquely impinging circular liquid jets" (Experimental Thermal and Fluid Science, V32) pp.1429-1439.
- [8] A. R. Kasimov, "A Stationary Circular Hydraulic jump, the limits of its existence and its Gas Dynamic Analogue" (Journal of Fluid Mechanics, 601, 2008) pp.189-198.
- [9] D. Sing, A. K. Das, "Computational Simulation of Radially Asymmetric Hydraulic Jump and Jump-Jump Interactions" (Computers and Fluids, Volume 170, 2018) pp.1-12.
- [10] M. J. Cho, B. G. Thomas, P. J. Lee, "Three-dimensional numerical study of impinging water jets in runout table cooling processes." (Metallurgical and Materials Transactions B, 2008) pp.593-602.
- [11] A. Duchesne, L. Lebon, L. Limat, "Constant Froude number in a circular hydraulic jump and its implication on the jump radius selection" (EPL, 107, 2014)
- [12] B. Mohajer, R. Li, "Circular hydraulic jump on finite surfaces with capillary limit." (Physics of Fluids, 27(11), 2015) pp.117102.
- [13] K. Choo and S. J. Kim, "The influence of nozzle diameter on the circular hydraulic jump of liquid jet impingement." (Experimental Thermal and Fluid Science, 72, 2016) pp.12-17.
- [14] V. C. Todkari and R. P. Kate, "Numerical and experimental investigations on a circular hydraulic jump due to normal impinging free liquid jet on a flat horizontal target plate." (Fluid Dynamics Research, 51(2), 2019) pp.025508.
- [15] H. Fujimoto, N. Hatta, and R. Viskanta, "Numerical Simulation of Convective Heat Transfer to a Radial Free Surface Jet Impinging on a Hot Solid" (Heat and Mass Transfer, vol. 35, 1999) pp. 266–272.
- [16] M. M. Rahman, A. J. Bula, and J. E. Leland, "Analysis of Turbulent Conjugate Heat Transfer to a Free Impinging Jet" (J. Thermophys. and Heat Transfer, vol. 14, 2000) pp.330–339.
- [17] "FLUENT® theory guide and user manual," ANSYS FLUENT® 14.5.
- [18] F. R. Menter, "Two-equation eddy-viscosity turbulence models for engineering applications" (AIAA-Journal, 32(8), 1994) pp. 1598-1605.
- [19] D. C. Wilcox, "Multiscale model for turbulent flows" (AIAA 24th Aerospace Sciences Meeting. American Institute of Aeronautics and Astronautics, 1986)
- [20] N. Zuckerman., N. Lior., "Jet impingement heat transfer: Physics, correlations and numerical modeling" (Advances in Heat Transfer, 39, 2006) pp. 565-631.
- [21] E. Dressaire, L. Courbin, J. Crest and H. A. Stone, "Inertia dominated thin-film flows over microdecorated surfaces" (Physics of Fluids, Volume 22, 2010)